Journal of Pediatric Neurology 7 (2009) 123–133
DOI 10.3233/JPN-2009-0292
IOS Press

Original Article

Ultrastructural pathology of human hydrocephalic cerebral cortex

Orlando J. Castejón*
Biological Research Institute, Zulia University, Maracaibo, Venezuela

Received 16 August 2008
Revised 10 January 2009
Accepted 1 February 2009

Abstract. The ultrastructural pathology of cerebral cortex in human hydrocephalus is described. Cortical biopsies of 17 patients of ages ranging from 10 days to 21 years old examined in our laboratory are described. Nerve cells show moderate and severe swelling characterized by dilation of endoplasmic reticulum canaliculi and perinuclear cistern, edema and degenerative changes of Golgi apparatus, variable degrees of mitochondrial swelling, and fragmentation of plasma membrane. The neighboring neuropil exhibits notable enlargement of extracellular space and signs of synaptic plasticity and degeneration. The astrocytes display edematous changes and phagocytic activity. Glycogen rich- and glycogen-depleted astrocytes are observed. Oligodendroglial cells appear normal in certain cases and in others show moderate hydropic changes. Numerous myelin figures are observed in some unidentified nerve cell processes. The capillary wall shows evident signs of blood-brain barrier dysfunction featured by increased endothelial vesicular and vacuolar transport, closed and open interendothelial junctions, and in severely edematous areas thinning and breakdown of capillary basement membrane. The role of ischemia, oxidative stress, increased calcium concentration, activation of N-methyl-d-aspartate (NMDA) receptors, and disturbance of ion homeostasis are discussed in relationship with the fine structural alterations of hydrocephalic brain parenchyma.

Keywords: Human hydrocephalus, nerve cell damage, synaptic plasticity, synaptic degeneration, reactive glial cells, extracellular space, electron microscopy

1. Introduction

Blockage of the cerebrospinal fluid (CSF) circulation in human hydrocephalus results in a rise in intraventricular pressure with dilation of the lateral ventricles, alterations on the fine structure of choroid plexus, and disruption of the ependymal lining. CSF is infused into the white matter through the damaged ependyma and causes severe periventricular edema, ependyma and periventricular white matter, cortical brain edema, parenchymal destruction, micro- and macrovascular changes, derangement of brain development, formation of cystic cavities, and reactive changes of glial cells. The subependymal white matter shows enlargement of extracellular space, edematous and degenerative changes in neurons, especially in axons and myelin sheath, edematous changes of glial cells, reactive astrocytosis and phagocytosis [1–15].

Since the pioneering work of Struck and Hemmer [9] very few studies have been dedicated to explore the human hydrocephalic cortical gray matter alterations. This aspect is basically important if we consider that CSF traverses the entire cerebral parenchyma as earlier demonstrated by Milhorat and Hammock [10] using

*Correspondence: Orlando J. Castejón, Instituto de Investigaciones Biológicas, "Drs. Orlando Castejón and Haydée Viloria de Castejón", Universidad del Zulia, Apartado 526, Maracaibo,Venezuela. Tel.: +58 261 7414370; E-mail: ocastejo@cantv.net; orlandocastejon@gmail.com.

isotope ventriculography in man. Foncin et al. [11] reported marked extracellular space in cortical biopsies of patients with normal pressure hydrocephalus. Castejón [12] found degenerative changes of neurons, glial cells, synaptic endings, enlargement of extracellular space, and blood-brain barrier disruption in infant patients with communicating hydrocephalus and Chiari malformation. Glees and Voth [13] found neuronal degenerative changes in biopsy material of hydrocephalic infants. Glees et al. [14] reported the fine structural features of the cerebral microvaculature in hydrocephalic human infants. Glees and Hasan [15] detailed some ultrastructural features of neuroglial cells in maturing hydrocephalic frontal cortex, such as proliferation of oligodendrocytes and vacuolation of microgliacytes. Del Bigio [16] postulated calcium-mediated proteolytic damage in the white matter of hydrocephalic rats. Del Bigio et al. [17], and Del Bigio [18] found in chronic hydrocephalus destruction of white matter of several regions of central nervous tissue associated with deficit of motor and cognitive functions. Castejón et al. [19] described oligodendroglial cell damage and demyelination in nenonate patients with congenital hydrocephalus. Castejón, Castejón and Castejón, and Castejón et al. [20–31] described the damage of nerve cell plasma membrane [20], Golgi complex derangement [21], glycogen-rich and glycogen-depleted astrocytes [22], mitochondrial changes [23], axonal and dendritic alterations [19,24], lysosome abnormalities [25], nerve cell nuclear and nucleolar changes [26], damage of dendritic spines [27], synaptic plasticity and synaptic degeneration [12,28,29], and nerve cell death in congenital hydrocephalus, and Chiari malformation [30].

The present study describes the fine structural alterations of human hydrocephalic cerebral cortex and emphasizes the neurodegeneration features induced by interstitial edema, and the associated ischemic process, which are closely related with the clinical symptoms observed in human hydrocephalus.

2. Materials and methods

Cortical biopsies of cerebral cortex of 17 neonate patients, infant and young patients with clinical diagnosis of congenital hydrocephalus, Chiari malformation, and postmeningitis hydrocephalus studied in our laboratory are illustrated in Table 1. Cortical biopsies were performed according to basic ethical principles of the Declaration of Helsinki. This study has been approved by the Ethical Committee of the Biological Research Institute and Policlinica Maracaibo. Table 1 contains the clinical data and lists the cortical regions from which the biopsies were taken. Two to five mm thick cortical biopsies were immediately fixed in the surgical room in 4% glutaraldehyde-0.1M phosphate or cacodylate buffer, pH 7.4 at 4°C. Later they were divided into 1 mm fragments and immersed in a fresh, similar solution for periods varying from 2 to 72 h, followed by secondary fixation in 1% osmium tetroxide-0.1M phosphate buffer, pH 7.4 for 1 hr. They were then rinsed for 5 to 10 min in a buffer similar to that used in the fixative solution, dehydrated in increasing concentrations of ethanol and embedded in Araldite or Epon. For proper orientation of the electron microscope study, thick sections of approximately 0.1 to 1 μm were stained with toluidine blue and examined with a Zeiss photomicroscope. Ultrathin sections obtained with a Porter-Blum and LKB ultramicrotomes were stained with uranyl acetate and lead citrate and observed in a JEOL 100B electron microscope. Observations were made using intermediate magnifications ranging from 24.000 to 75.000 X.

3. Results

3.1. Intracellular edema of hydrocephalic nerve cells

In the cortical biopsies examined in our laboratory the laminar structure of cerebral cortex is well preserved by gluraldyhide-osmiun fixation immersion technique. Focal cortical dysplasia with persistent fetal radial columnar architecture of disorganized cortex with displaced neurons are not observed. In pyramidal and non-pyramidal neurons, moderate to severe swelling of intraneuronal compartment revealed by plasma membrane fragmentation, variable degrees of enlargement of rough endoplasmic reticulum and perinuclear cisterns, and wide communications between the nucleoplasm and cytoplasmic matrix are constantly found. A degranulated rough endoplasmic reticulum also is observed [12]. The intracellular edema is prominent at the level of the smooth Golgi flattened stacked cisterns, which appear extremely dilated and fragmented [21]. The mitochondria exhibit also a wide spectrum of morphological changes ranging from light to moderate and severe swelling, with clear and dense matrix, and fragmented cristae. Some mitochondria appear degenerated [23]. Electron dense spheroids, stacking or whorling of cristae, and paracristallin structures are not observed. Lysosomes show damage of their limiting

Table 1
Human hydrocephalus. Neurosurgical study

Case number	Age/Sex	Clinical data	Diagnosis	Cortical biopsy
1	1 month/ Female	Increased cephalic circumference, dysjunction of sutures, tense fontanelles	Uncompensated communicating congenital hydrocephalus	Right parietal cortex
2	1 month/ Female	Increased cephalic circumference, poor feeding, tense fontanelles	Uncompensated congenital hydrocephalus	Right temporo-parietal cortex
3	1 month/ Female	Increased cephalic circumference, hypertensive fontanelles, vomiting, dysjunction of sutures	Congenital communicating hydrocephalus	Right frontal cortex
4	6 months/ Male	Increased cephalic circumference, dysjunction of sutures, tense fontanelles, left peridural abscess	Congenital hydrocephalus	Right temporo-parietal cortex
5	10 days/ Male	Bulging of fontanelles and increased cephalic circumference after surgical correction of lumbar meningomyelocele	Chiari malformation type II, communicating hydrocephalus	Frontal cortex
6	2 months/ Female	Increased cranial volume, hypertensive fontanelles, deviation of gaze to the right, external rotation of both legs and increased tendinous reflexes after treatment of meningomyelocele	Chiari malformation type II, hydrocephalus, parieto-occipital intraparenchymatous abscess	Right parietal cortex
7	12 days/ Female	Increased cephalic circumference after treatment of lumbar meningomyelocele	Congenital hydrocephalus, meningomyelocele (Chiari type II)	Right parietal cortex
8	3 months/ Male	Febrile syndrome, meningitis, obstructive hydrocephalus after 2 weeks	Postmeningitis hydrocephalus	Right frontal cortex
9	8 months/ Female	Increased cranial volume since 3 months of age, tense fontanelles, poor feeding.	Congenital communicating hydrocephalus	Right parietal cortex
10	3 months/ Male	Meningeal syndrome, tonic-clonic convulsions, increased cephalic circumference, vomiting, increased limb tone.	Postmeningitis hydrocephalus	Right frontal cortex
11	4 months/ Female	Increased cephalic circumference, hypertensive fontanelles.	Congenital hydrocephalus	Right frontal central cortex
12	3 months/ Male	Increased cephalic circumference observed 1 month after birth.	Communicating hydrocephalus	Right frontal cortex
13	2 years/ Female	Increased cranial volume since 4 months of age.	Comumunicating hydrocephalus	Right frontal cortex
14	7 months/ Male	Increased cranial volume, diagnosis of subarachnoid hemorrhage after computed axial tomography.	Communicating hydrocephalus	Right frontal cortex
15	4 months/ Female	Increased cephalic circumference. Dysjunction of sutures. Tense fontanelles.	Pinealoma of third ventricle	Posterior parietal cortex
16	21 years/ Male	Sudden increase of cephalic circumference, tonic convulsions.	Pinealoma of third ventricle	Posterior parietal cortex
17	5 years/ Female	Increased cephalic circumference.	Communicating hydrocephalus	Right parietal cerebral cortex

plasma membrane, and appear surrounded by areas of cytoplasmic focal necrosis [25] (Figs 1 and 2).

The hydropic changes of nuclear and cytoplasmic matrix induce an increased electron lucent aspect of nerve cells, which acquired a watery appearance. The edematous and degenerative changes of cerebral cortex in human hydrocephalus appeared to be initially of a mechanical origin due to the high CSF pressure, and secondarily to the increased interstitial edema, ischemic process, and oxidative stress [12]. In addition to the neuronal edema there is also an associated ischemic process. The role of ischemia in neonatal brain injury was formerly suggested by Del Biggio et al. [8].

3.2. *Pathology of myelinated axons*

A myelination delay and damage of myelinated axons featured by myelin sheath vacuolation and derangement of cytoskeletal structures are observed in the white and gray matter [1,5,7–9,11,12,17,18]. Myelinated axons are not observed in the neonate patients with congenital hydrocephalus, especially in those patients between 10 days and 3 months of age [19].

3.3. *Electron microscopic changes of dendrites in congenital hydrocephalus*

The immature hydrocephalic cerebral cortex neuropil in neonate patients with congenital hydrocephalus

Fig. 1. Congenital hydrocephalus. Right parietal cortex. Case no. 1. A 1-month-old female neonate. Non-pyramidal neuron exhibiting fragmented plasma membrane (long arrow), distended endoplasmic reticulum cisterns (ER), detachment of membrane associated ribosomes (short arrows), and disassembly of some nuclear pores (arrowheads). The mitochondria (M) appear swollen. Note the enlarged extracellular space in the neighboring neuropil (asterisks).

Fig. 2. Chiari Type II malformation. Hydrocephalus. Frontal cortex. Case no. 5. A 10-day-old male neonate. Edematous non-pyramidal neuron showing lysosomes (L) and a multivesicular body (MB) with disrupted limiting membranes (arrows). Note the clear edematous mitochondria (M), and the dilated rough endoplasmic reticulum embedded in an electron lucent cytosol.

shows irregularly beaded shaped, and swollen and vacuolated dendritic processes with elongated and dark mitochondria. Some of them exhibit lamellipodic and filopodic processes, and endocytic vesicle formation at the limiting plasma membrane. Some dendritic processes show fragmented plasma membrane in areas of severe brain edema [24] (Fig. 3).

3.4. *Dendritic spine abnormalities in congenital hydrocephalus*

In patients with congenital hydrocephalus and Chiari type II malformation, a variety of swollen spine shapes are found such as mushroom type-, filopodic and lanceolate spines [27]. Some of these spines exhibit the spine apparatus, featured by closely applied endoplasmic sacs, which allow to differentiate from axonal growth cones (Fig. 4).

In the immature neuropil of these neonate and hydrocephalic patients, some spines appear axonless or unattached, and others making asymmetric axodendritic synaptic contacts. The immature spines exhibit mostly an elongated neck with several microtubules. Unattached or axonless elongated spines presumably represent a compensatory mechanism to navigate in the widened extracellular space of the immature neuropil to reach axons farther away. These spines exhibit an edematous head, a disrupted actin-like network, dilated profiles of smooth endoplasmic reticulum, swollen clear and dense mitochondria, and clusters of free ribosomes. Such alterations are due to dendrotoxicity. Some congenital hydrocephalus exhibited megaspines (Fig. 5), with one or two synaptic active zones. These megaspines, most of them about 2.86 μm in length, contain an edematous spine apparatus, and exhibit a long neck with degenerated microtubules [27].

3.5. *Synaptic plasticity and degeneration in congenital hydrocephalus*

In human congenital hydrocephalus synaptic plasticity is characterized by the presence of activated flat and invaginated axodendritic and axospinodendritic asymmetric synaptic contacts showing synaptic vesicles anchored to the presynaptic membrane, and short or large synaptic active zones. In addition, swollen and degen-

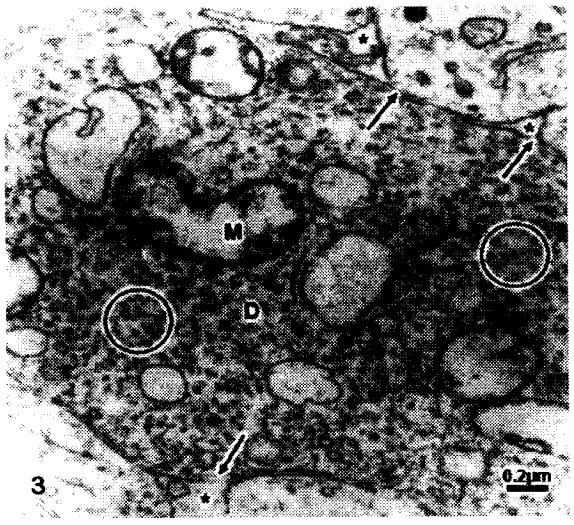

Fig. 3. Chiari Type II malformation. Hydrocephalus. Right parietal cortex. Case no. 6. A 2-month-old female infant. Segment of the longitudinal section of an edematous dendritic process (D) showing a clear dendroplasm with cross sectioned microtubules and neurofilaments (circles). The long arrows label the disrupted dendritic plasma membrane. Note the dilated extracellular space (asterisks) surrounding the dendritic profile that features hydrocephalus interstitial edema.

Fig. 4. Chiari Type II malformation. Hydrocephalus. Case no. 7. A 12-day-old female neonate. Neuropil of right parietal cortex showing the presence of a lanceolate and axonless spine exhibiting a long neck (long arrows), a dark mitochondrion (M) and free ribosomes (circle). An edematous spine head (short arrows) is observed making asymmetric synapse with a presynaptic ending (PE), and exhibiting a dilated endoplasmic reticulum profile (ER). Another small axonless spine (S) is seen. The hydrocephalic edema at the extracellular spaces is labeled with asterisks.

erated axodendritic and axosomatic synaptic contacts exhibit enlargement of few synaptic vesicles and lack of pre- and post synaptic densities [28,29] (Fig. 6).

Beside, isolated and swollen presynaptic endings with few or numerous synaptic vesicles, disruption of limiting plasma membrane, and without postsynaptic partners are observed. Synaptic disassembly occurs in elevated intracranial pressure-hydrocephalus (Fig. 7). Phagocytic astrocytes appear engulfing the degenerated synapses. Hydrocephalic edema and ischemia, oxidative stress, increased calcium concentration, activation of N-methyl-d-aspartate (NMDA) receptors, and disturbance of ion homeostasis are apparently related with the synaptic plasticity and synaptic degenerative changes observed in human hydrocephalus [28,29].

The damage of nerve cell processes and synaptic contacts indicates nerve cell circuit alterations in the hydrocephalic cortex, which might explain some clinical and neurological symptoms, such as decline in intellectual functions and learning disabilities, behavior changes, motor deficits, and seizures observed in infant hydrocephalic patients [1,12,13,17].

3.6. Reactive and hydropic changes and phagocytic activities of glial cells

Two distinct morphological types of astrocytes: Glycogen rich- and glycogen depleted astrocytes in congenital hydrocephalus have been found in human congenital hydrocephalus (Figs 8 and 9). They are observed in perineuronal, neuropil and perivascular localization. These findings suggest astrocytic glycogen mobilization during anoxic and ischemic conditions, revealing the important contribution of astrocytes on neuronal survival under conditions of energy substrate limitations. Astroglial cells might perform several energy-dependent functions that may aid neuronal and oligodendroglial cell survival in pathological conditions, such as congenital hydrocephalus [22].

At the level of cortical gray matter neuropil, the astrocyte cells show notable edematous changes and phagocytic activity [30]. Gliosis and microgliosis have been reported to be a common and persistent feature in the white matter of hydrocephalic brain [15,32].

In the edematous human cortical gray matter, the oligodendroglial cells exhibit in certain regions a normal structural pattern, and in severely edematous areas moderate and remarkably hydropic changes leading to oncotic cell death [19,30] (Fig. 10).

Fig. 5. Congenital hydrocephalus. Right frontal cortex. Case no. 8. A 3-month-old male infant. Neuropil of right parietal cortex showing a megaspine (MS), exhibiting a long neck (short arrows) and two asymmetric synaptic contacts (long arrows) with swollen presynaptic endings (PE). The spine head shows a disrupted actin-like network (circle), an atrophic spine apparatus (arrowheads), and a clear swollen mitochondrion (M). The asterisks label the enlarged hydrocephalic extracellular space.

3.7. *Presence of myelin figures*

Numerous myelin figures are observed in nerve cells and astrocytes in human congenital hydrocephalus, suggesting that the pressure exerted by the interstitial edema, and the anoxic ischemic conditions of brain parenchyma induce the concentrically arrangement of nerve cell cytomembranes. Apparently these concentric lamellar formations are conformational changes induced by the high pressure exerted by the non-circulating CSF present in the dilated extracellular space upon the immature plasma membranes, which have distinct macromolecular composition, characterized by changes in integral membrane proteins, cholesterol domains, and in certain carbohydrates residues and anionic sites [33].

Fig. 6. Congenital hydrocephalus. Right frontal cortex. Case no. 10. A 3-month-old male infant. Immature axosomatic synaptic contact (long arrow) on a swollen non-pyramidal neuron (NP) showing enlarged and clear synaptic vesicles, and absence of pre- and postsynaptic densities. Another immature axodendritic contacts (short arrows) also are distinguished.

3.8. *Blood brain barrier dysfunction*

The capillary wall shows evident signs of blood-brain barrier dysfunction characterized by increased endothelial vesicular and vacuolar transport (Fig. 11), closed and open interendothelial junctions, thin and fragmented basement membrane with areas of focal thickening, and discontinuous perivascular astrocytic end-feet. In severely edematous areas with presence of disrupted neuropil, the perivascular space is notably enlarged and the capillaries appeared floating as isolated structures. They show tight or partially open endothelial junctions, increased vesicular and vacuolar transendothelial transport, and swollen and disrupted basement membrane. Our findings in human hydrocephalus favor the idea of an interendothelial route either for edema formation or resolution in human hydrocephalic cerebral cortex [34].

Glees et al. [14] studying the microvasculature in hydrocephalic human infants have also postulated a possible role of endothelial pinocytotic vesicle as a transcellular route for hydrocephalic edema resolution and considered that CSF or edema fluid is absorbed into the vascular system via a transendothelial pathway. Hasan and Glees [35] have postulated a possible role of

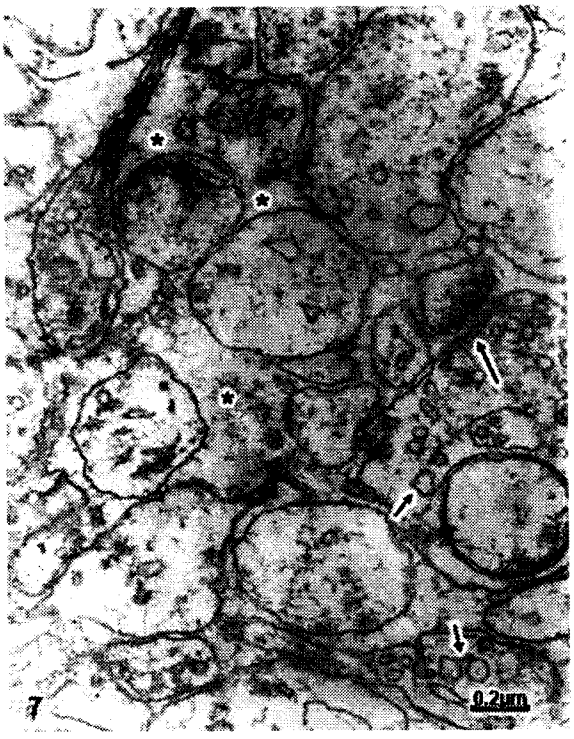

Fig. 7. Congenital communicating hydrocephalus. Right frontal cortex. Case no. 12. A 3-month-old male infant. Severely edematous neuropil showing synaptic disassembly (long arrow). The pre-and postsynaptic endings appear separated by a notably dilated synaptic cleft. The swollen presynaptic endings (short arrows) exhibit enlarged synaptic vesicles. Note the over-distended extracellular space (asterisks) suggesting that the severe hydrocephalic edema induced synaptic disassembly.

perivascular pericytes and juxtavascular phagocytes in hydrocephalic edema resolution. In an early publication [36] we have reported that pericytes also exhibit remarkable edematous changes, increased vesicular and vacuolar transport, formation of transient transpericytal channels, and tubular structures in human congenital hydrocephalus.

3.9. The hydrocephalic or interstitial edema

The neighboring neuropil formed by an intricate complex of neuronal and neuroglial cell processes shows notable enlargement of the electron lucid and preexisting extracellular space located among these processes (Figs 1, 3, 4 and 11), which is occupied by the non-proteinaceous and non-circulating CSF [37, 38]. The enlargement of the extracellular space is more evident than the dilation of the intracellular space. Lacunar extracellular spaces are constantly found at the meeting point of three or four nerve cell processes. The

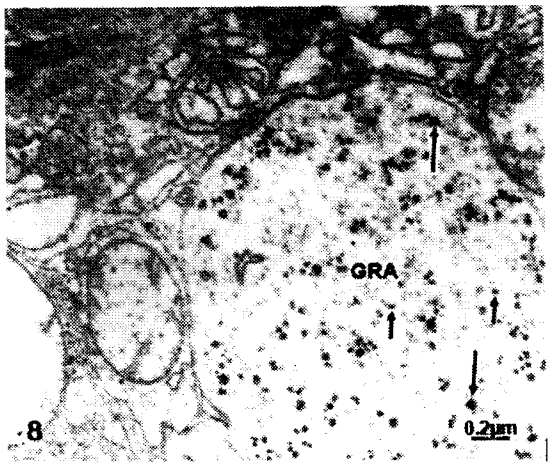

Fig. 8. Chiari Type II malformation. Hydrocephalus. Case no. 7. Right parietal cortex. A 12-day-old female neonate. Swollen glycogen-rich astrocytic cytoplasm (GRA) showing alpha- (long arrows) and beta- types (short arrows) glycogen granules.

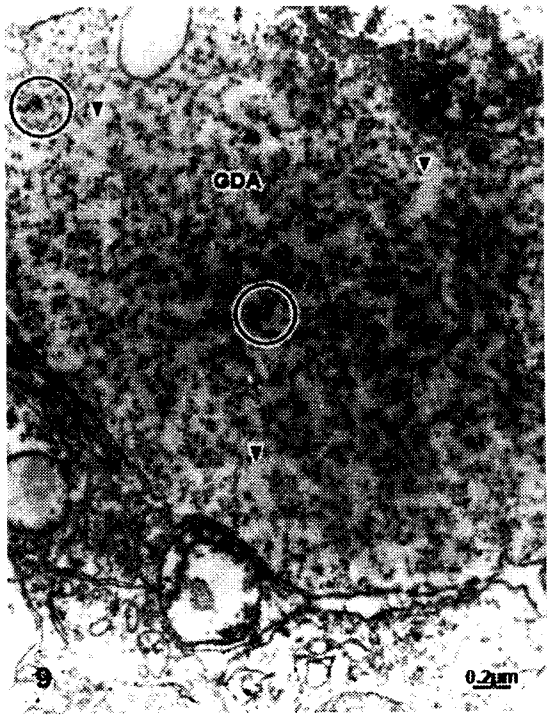

Fig. 9. Congenital hydrocephalus. Right frontal cortex. Case no. 10. A 3-month-old male infant. Glycogen-depleted astrocyte (GDA) showing an electron lucent cytoplasmic matrix, few dispersed glycogen granules (circles) surrounded by high clear spaces (arrowheads) previously occupied by the mobilized glycogen granules.

pressure of the extracellular non-circulating CSF induces separation, indentation and rupture of nerve cell processes. Similar observations were earlier reported

Fig. 10. Chiari Type II malformation. Communicating hydrocephalus. Frontal cortex. Case no. 5. A 5-day-old male neonate. Severely edematous oligodendroglia cell (OL) leading to oncotic cell death featured by wide communications between the perinuclear cistern and rough endoplasmic reticulum (arrows) and the extracellular space (asterisks). Note the decondensed state of nuclear euchromatin (EC) featured by granular and fibrillar organization (arrowheads).

Fig. 11. Congenital hydrocephalus. Right frontal cortex. A 4-month-old female infant. Longitudinally sectioned capillary showing dark endothelial cells (EC) exhibiting large vacuoles (V), a closed endothelial junction (EJ), a fine basement membrane (BM) with focal thickenings, and attached glycogen rich- and glycogen depleted perivascular astrocytic end-feet (GR,GD). Note the enlarged perivascular space (asterisks).

by Struck and Hemmer [9], and Foncin et al. [11] on the gray matter of human hydrocephalus. The increased extracellular space of human cortical neuropil suggests the establishment of a transparenchymal route for fluid absorption through the cortical capillaries.

The penetration of CSF induces edematous and degenerative changes in the neighboring neurons, neuroglial cells and synaptic regions. The damage of the gray matter results from both hydrostatic forces and biochemical alterations induced by the extracellular pooling of CSF, and also by the expansion forces or stretching effect produced by the ventricular enlargement [12,37,38].

3.10. Nerve cell death in human hydrocephalus

In human congenital hydrocephalus, non-pyramidal neurons undergo a coexisting oncotic and apoptotic process, characterized by cytoplasmic and plasma membrane blebbing, remarkably swollen mitochondria and endoplasmic reticulum canaliculi and cisterns [30]. According to Majno and Joris [38], and Trump et al. [39] these features have been characterized as oncosis. Nerve cells suffering a clear apoptotic process also are found characterized by chromatin condensation and formation of typical apoptotic bodies. Some nerve cells exhibit a combined process of oncosis and apoptosis. Both types of combined nerve cell death were considered as leading to necrosis. This later conceptualized as the changes that occur after nerve cell death [30,39]. Although oncosis, apoptosis and necrosis are mediated through distinct pathways, in human hydrocephalus we have found a continuum process of oncosis, apoptosis and necrosis, depending of the severity of brain edema parenchyma, the age of the patients, and the moderate or severe anoxic-ischemic conditions involved [30]. The astrocytes also show a combined oncotic and apoptotic cell death featured by strong chromatin condensation, disrupted swollen cytoplasm and fragmented limiting plasma membranes. These hybrid forms of astrocyte cell death also lead to necrosis (Fig. 12).

Fig. 12. Congenital communicating hydrocephalus. Right parietal cortex. Case no. 17. A 5-year-old female patient. Fibrous astrocyte (A) showing a combined oncotic and apoptotic cell death process leading to necrosis characterized by a disrupted and swollen cytoplasm, and a fragmented plasma membrane communicated with the enlarged extracellular space (long arrows). Note the shrunken lobulated nucleus (N), and the strong chromatin condensation (CC).

The oligodendrocyte cells exhibit mainly oncotic cell death featured by a decondensed nuclear chromatin, enlarged and disrupted perinuclear cistern widely communicated with the endoplasmic reticulum and the dilated extracellular space, suggesting that the oncotic cell death is due to the high pressure exerted by the interstitial hydrocephalic edema or probably occurring in areas with milder forms of ischemic damage [30].

In congenital hydrocephalus and Chiari malformations we are dealing with immature brains, where oncosis, apoptosis and necrosis also occur as a continuum, as previously described by Portera-Cailliau et al. [40] and Martin [41] in inmmature brain parenchyma. In these cases the nerve cell populations exhibit high vulnerability, and support the hypothesis that excitotoxic neuronal death in the immature brain is not an uniform event [40], but rather overlapped morphological processes, with a distinct phenotype of neurodegeneration. Autophagic cell death has not been reported until now in human hydrocephalus.

The nerve cell death in congenital hydrocephalus is related with the severity of brain edema, anoxic-ischemic conditions of brain parenchyma, oxidative stress, glutamate excitotoxicity, calcium overload, and caspase dependent and independent mechanisms [42–45].

3.11. Fixation artifacts versus real hydrocephalic pathology

A careful fixation protocol of human cortical biopsies was used to avoid fixation artifacts. The cortical biopsies were immediately placed in glutaraldehyde fixative solution by the neurosurgeon at the surgical room to avoid delay fixation. Instrumental manipulation, pressure and excessive handling of the brain sample were avoided. Once the cortical biopsy arrived at the Electron Microscopy Laboratory the samples were placed in new and similar fixatives to avoid fixation artifacts introduced by inactivation of fixative solution by the remaining blood present in the sample. This procedure proved to be the best for optimal fixation of human cortical biopsies. Samples with poor fixation were discarded. Poor fixation gave images that superimposed to hydrocephalic edema resulting in drastic changes of nerve cell electron microscopic morphology than can be clearly differentiated from real hydrocephalic pathology. In areas of moderate brain interstitial edema normal and swollen mitochondria were simultaneously observed indicating optimal fixation procedure.

4. Conclusions

Hydrocephalic nerve cells exhibit intracellular edema characterized by dilation of endoplasmic reticulum canaliculi and perinuclear cistern, areas of degranulated rough endoplasmic reticulum, edema and degenerative changes of Golgi apparatus, variable degrees of mitochondrial swelling, lysosomal damage, and fragmented limiting plasma membrane. Myelination delay, myelin sheath vacuolation, cytoskeletal derangement, and oligodendroglial cell damage are found. Myelinated axons are not observed in some hydrocephalic neonate patients. The dendrites show edematous changes, irregularly beaded shaped, and swollen and vacuolated dendritic processes with elongated and dark mitochondria. A variety of swollen spine shapes are found such as mushroom type, filopodic and lanceolate

spines. Some spines appear axonless or unattached, and others are making asymmetric axodendritic synaptic contacts. Signs of synaptic plasticity and synaptic degeneration are simultaneously observed. Megaspines also are distinguished. The damage of nerve cell processes and synaptic contacts indicates nerve cell circuit alterations in the hydrocephalic cortex, which might explain some clinical and neurological symptoms, such as decline in intellectual functions and learning disabilities, behavior changes, motor deficits, and seizures observed in infant hydrocephalic patients. Hydrocephalic edema and ischemia, oxidative stress, increased calcium concentration, activation of NMDA receptors, and disturbance of ion homeostasis are apparently related with the synaptic plasticity and synaptic degenerative changes observed in human hydrocephalus. Astrocyte cells show notable edematous changes and phagocytic activity. Glycogen rich- and glycogen depleted astrocytes are found in congenital hydrocephalus. These findings suggest astrocytic glycogen mobilization during anoxic and ischemic conditions, revealing the important contribution of astrocytes on neuronal survival under conditions of energy substrate limitations. The capillary wall shows evident signs of blood-brain barrier dysfunction characterized by increased endothelial vesicular and vacuolar transport, closed and open interendothelial junctions, thin and fragmented basement membrane with areas of focal thickening, and discontinuous perivascular astrocytic end-feet layer. The perivascular space is notably dilated and widely communicated with the enlarged extracellular space in the neuropil. The increased extracellular space of the human cortical neuropil suggests the establishment of a transparenchymal route for fluid absorption through the cortical capillaries. In human congenital hydrocephalus, non-pyramidal neurons and astrocytes undergo a coexisting oncotic and apoptotic process leading to necrosis. Oligodendrocyte cells exhibit mainly oncotic cell death. The nerve cell death in congenital hydrocephalus is related with the severity of brain edema, anoxic-ischemic conditions of brain parenchyma, oxidative stress, glutamate excitotoxicity, calcium overload, and caspase dependent and independent mechanisms.

Acknowledgement

This paper has been carried out from a subvention obtained of CONDES-LUZ. Zulia University. Maracaibo. Venezuela.

References

[1] R.O. Weller and K. Shulman, Infantile hydrocephalus: clinical, histological, and ultrastructural study of brain damage, *J Neurosurg* **36** (1972), 255–265.

[2] D.L. Price, E. James, E. Sperber and E.P. Strecker, Communicating hydrocephalus. Cisternographic and neuropathologic studies, *Arch Neurol* **33** (1976), 15–204.

[3] C.M. Bannister and S.A. Chapman, Ventricular ependyma of normal and hydrocephalic subjects: a scanning electronmicroscpic study, *Dev Med Child Neurol* **22** (1980), 725–735.

[4] M. Del Bigio, J.E. Bruni and H.D. Fewer, Human neonatal hydrocephalus. An electron microscopic study of the periventricular tissue, *J Neurosurg* **63** (1985), 56–63.

[5] K. Akai, S. Uchigasaki, U. Tanaka and A. Komatsu, Normal pressure hydrocephalus. Neuropathological study, *Acta Pathol Jpn* **37** (1987), 97–110.

[6] J.J. Volpe, Intraventricular hemorrhage and brain injury in the premature infant, Neuropathology and pathogenesis, *Clin Perinatol* **16** (1989), 361–386.

[7] M.R. Del Bigio, Neuropathological changes caused by hydrocephalus, *Acta Neuropathol* **85** (1993), 573–585.

[8] M.R. Del Bigio, M.C. da Silva, J.M. Drake and U.I. Tuor, Acute and chronic cerebral white matter damage in neonatal hydrocephalus, *Can J Neurol Sci* **21** (1994), 299–305.

[9] G. Struck and R. Hemmer, Electron microscopic studies on the human cerebral cortex in hydrocephalus, *Arch Psychiatr Nervenkr* **206** (1964), 17–27 (in German).

[10] T.H. Milhorat and M.K. Hammock, Isotope ventriculography. Interpretation of ventricular size and configuration in hydrocephalus, *Arch Neurol* **5** (1971), 1–8.

[11] J.F. Foncin, A. Redondo and J. LeBeau, Cerebral cortex in normal pressure hydrocephalus: an electron microscopy study, *Acta Neuropathol* **34** (1976), 353–357 (in French).

[12] O.J. Castejón, Transmission electron microscope study of human hydrocephalic cerebral cortex, *J Submicrosc Cytol Pathol* **26** (1994), 29–39.

[13] P. Glees and D. Voth, Clinical and ultrastructural observations of maturing human frontal cortex, Part I (Biopsy material of hydrocephalic infants), *Neurosurg Rev* **11** (1988), 273–278.

[14] P. Glees, M. Hasan, D. Voth and M. Schwarz, Fine structural features of the cerebral microvaculature in hydrocephalic human infants: correlated clinical observations, *Neurosurg Rev* **12** (1989), 315–321.

[15] P. Glees and M. Hasan, Ultrastructure of human cerebral macroglia and microglia: maturing and hydrocephalic frontal cortex, *Neurosurg Rev* **13** (1990), 231–242.

[16] M.R. Del Bigio, Calcium-mediated proteolytic damage in white matter of hydrocephalic rats? *J Neuropathol Exp Neurol* **59** (2000), 946–954.

[17] M.R. Del Bigio, W.J. Wilson and T. Enno, Chronic hydrocephalus in rats and humans: white matter loss and behavior changes, *Ann Neurol* **53** (2003), 337–346.

[18] M.R. Del Bigio, Cellular damage and prevention in childhood hydrocephalus, *Brain Pathol* **14** (2004), 317–324.

[19] O.J. Castejón, H.V. Castejón and A. Castellano, Oligodendroglial cell damage and demyelination in infant hydrocephalus. An electron microscopy study, *J Submicrosc Cytol Pathol* **33** (2001), 33–40.

[20] O.J. Castejón, Ultrastructural pathology of neuronal membranes in the oedematous cerebral cortex, *J Submicrosc Cytol Pathol* **36** (2004), 167–179.

[21] O.J. Castejón, Ultrastructural pathology of Golgi apparatus of nerve cells in human brain edema associated to brain congen-

ital malformations, tumours and trauma, *J Submicrosc Cytol Pathol* **31** (1999), 203–213.

[22] O.J. Castejón, M. Diaz, H.V. Castejón and A. Castellano, Glycogen-rich and glycogen-depleted astrocytes in the oedematous human cerebral cortex associated with brain trauma, tumours and congenital malformation: an electron microscopy study, *Brain Injury* **16** (2002), 109–132.

[23] O.J. Castejón and H.V. Castejón, Structural patterns of injured mitochondria in human oedematous cerebral cortex, *Brain Inj* **18** (2004), 1107–1126.

[24] O.J. Castejón and G.J. Arismendi, Morphological changes of dendrites in the human edematous cerebral cortex, A transmission electron microscopic study, *J Submicrosc Cytol Pathol* **35** (2003), 395–413.

[25] O.J. Castejón, Lysosome abnormalities and lipofucsin content of nerve cells of oedematous human cerebral cortex, *J Submicrosc Cytol Pathol* **36** (2004), 263–271.

[26] O.J. Castejón and G.J. Arismendi, Nerve cell nuclear and nucleolar abnormalities in the human oedematous cerebral cortex, An electron microscopic study using cortical biopsies, *J Submicrosc Cytol Pathol* **36** (2004), 273–283.

[27] O.J. Castejón, A. Castellano and G. Arismendi, Transmission electron microscopy of cortical dendritic spines in the human oedematous cerebral cortex, *J Submicrosc Cytol Pathol* **36** (2004), 181–191.

[28] O.J. Castejón, Synaptic plasticity in the oedematous human cerebral cortex, *J Submicrosc Cytol Pathol* **35** (2003), 177–179.

[29] O.J. Castejón, Synaptic plasticity and synaptic degeneration in human congenital hydrocephalus, *J Pediatr Neurol* **6** (2006), 99–107.

[30] O.J. Castejón and G.J. Arismendi, Nerve cell death types in the edematous human cerebral cortex, *J Submicrosc Cytol Pathol* **38** (2006), 21–36.

[31] O.J. Castejón, *Electron Microscopy of Human Brain Edema*, Collections of Zulia University Books, Maracaibo, Venezuela, Astrodata, 2008.

[32] F.T. Mangano, J.P. McAllister, 2nd, H.C. Jones, M.J. Johnson and R.M. Kriebel, The microglial response to progressive hydrocephalus in model of inherited aqueductal stenosis, *Neurol Res* **20** (1998), 697–704.

[33] L. Surchev, V. Dontchev, K. Ichev et al., Changes in the neuronal plasma membrane during synaptogenesis, *Cell Mol Biol (Noisy-le-grand)* **41** (1995), 1073–1080.

[34] O.J. Castejón, Blood-brain barrier ultrastructural alterations in human congenital hydrocephalus and Arnold- Chiari malformation, *Folia Neuropathol* **49** (2009) (in press).

[35] M. Hasan and P. Gilees, The fine structure of human cerebral perivascular pericytes and juxtavascular phagocytes: their possible role in hydrocephalic edema resolution, *J Hirnforsch* **31** (1990), 237–249.

[36] O.J. Castejón, Submicroscopic changes of cortical capillary pericytes in human perifocal brain edema, *J Submicrosc Cytol* **16** (1984), 601–618.

[37] O.J. Castejón, A. Castellano, G.J. Arismendi and Z. Medina, The inflammatory reaction in human traumatic oedematous cerebral cortex, *J Submicrosc Cytol Pathol* **37** (2005), 43–52.

[38] G. Majno and I. Joris, Apoptosis, oncosis, and necrosis. An overview of cell death, *Am J Pathol* **146** (1995), 3–15.

[39] B.F. Trump, I.K. Berezesky, S.H. Chang and P.C. Phelps, The pathways of cell death: oncosis, apoptosis, and necrosis, *Toxicol Pathol* **25** (1997), 82–88.

[40] C. Portera-Cailliau, D.L. Price and L.J. Martin, Excitotoxic neuronal death in the immature brain is an apoptosis-necrosis morphological continuum, *J Comp Neurol* **378** (1997), 70–87.

[41] L.J. Martin, Neuronal cell death in nervous system development, disease, and injury (Review), *Int J Mol Med* bf 7 (2001), 455–478.

[42] D.J. Socci, K.B. Bjugstad, H.C. Jones, J.V. Patisapu and G.W. Arendash, Evidence that oxidative stress is associated with the pathophysiology of inherited hydrocephalus in the H-Tx rat model, *Exp Neurol* **155** (1999), 109–117.

[43] L. Annunziato, S. Amoroso, A. Pannaccione et al., Apoptosis induced in neuronal cells by oxidative stress: role played by caspases and intracellular calcium ions, *Toxicol Lett* **139** (2003), 125–133.

[44] S.P. Cregan, A. Fortin, J.G. MacLaurin et al., Apoptosis-inducing factor is involved in the regulation of caspase-independent neuronal cell death, *J Cell Biol* **158** (2002), 507–517.

[45] Q. Chen, Y.C. Chai, S. Mazumder et al., The late increase in intracellular free radical oxygen species during apoptosis is associated with cytochrome c release, caspase activation, and mitochondrial dysfunction, *Cell Death Differ* **10** (2003), 323–334.